CHAPTER 4 submitted to Marine and Petroleum Geology

Origin of marine petroleum source rocks from the Late Jurassic/Early Cretaceous Norwegian Greenland Seaway – evidence for stagnation and upwelling

U. Langrock and R. Stein

Alfred Wegener Institute for Polar and Marine Research, Department of Geosciences, Columbusstrasse, 27568 Bremerhaven, Germany

Abstract

Forty samples were selected from Late Jurassic to early Cretaceous black shales of IKU sites 6307/07-U-02 and 6814/04-U-02, located on the mid-Norwegian shelf, for a detailed maceral analysis. The penetrated rocks include the *Spekk* and *Hekkingen* formations, which represent major potential petroleum source rocks in the region. It was our first objective to reveal the type of organic material that has produced the source rock potential of these sediments. The results suggest that black shale formation has occurred in two different paleoceanographic settings, i.e. in a "high-productive" and an "anoxic/stagnant" environment, which was supported by inorganic and sedimentological data. In addition, new data for estimating sedimentation rates (SR) gave impulse for using accumulation rates to access the authentic organic carbon flux to the sediment. Organic carbon accumulation rates are relatively low but similar to mid-Cretaceous black shales from other ocean areas (average 10 – 300 mg/cm^2/ka). Supported by redox-sensitive Re/Mo ratios, SR/TOC relationships, and paleoproductivity estimates we suggest that black shale formation in the *Spekk Formation* has followed largely the conditions of the “stagnation model”, whereas the *Hekkingen Formation* is likely an example for the “productivity model”.

4.1. Introduction

The geological understanding of the middle and upper Norwegian shelf (Fig. 4-1) has been improved largely by prospective and explorative operations during the 1980s and early 1990s and is summarized in drilling reports and subsequent papers, e.g. by Skarbø et al. (1988), Worsley et al. (1988), Hansen et al. (1991), Leith et al. (1990), Jongepier et al. (1996). Modern insights in plate tectonic evolution, structural properties, sedimentology, paleoceanography, and geochemistry of late Mesozoic strata along the Norwegian shelf, including sediments of commercial importance, are owing to these investigations (e.g. Brekke et al., 1999; Smelror et al., 2001; Swientek and Ricken, 2002; Lipinski et al., 2003; Langrock et al., in press; Mutterlose et al., 2003). Late Jurassic to Early Cretaceous fine-grained sediments crop up along the eastern margin of the Norwegian-Greenland-Seaway and adjacent marginal seas (Smelror et al., 1994; Leith et al., 1990; Worsley et al., 1988; Århus et al., 1991; Wagner and Hölemann, 1995; Doré, 1991; Doré et al., 1997; Bugge et al., 2002; Mutterlose et al., 2003; Langrock et al., 2003). Drilling also recovered sediments that are exceptionally rich in organic carbon and provide moderate to very good source rock potential for liquid and gaseous petroleum. We investigated sediments from the mid-Norwegian shelf (Fig. 4-1) that represent major potential petroleum source rocks in the region. The cores are characterized by two major lithological units, including the *Spekk* and *Hekkingen* formations (Fig. 4-2). A thick sequence of dark-colored, organic carbon-rich claystones (i.e. black shales) with subordinate silty or calcareous intercalation dominates the lower part of the cores, which is followed by a sequence of light-colored or reddish organic carbon-poor siltstones, marls and limestones. The transition between these two sedimentary units occurred gradually within a time interval of about 10 My during the Berriasian and Valanginian. The late Jurassic black shale sequences are represented by the *Spekk* Formation, which is a major source rock west of the Vøring Marginal High between 62° and 68° N (Fig. 4-1) and the time-equivalent *Hekkingen* Formation, which is an important source rock in the Nordland and Troms areas and extends into the central Barents Sea (e.g. Bugge et al., 1989, 2002; Worsley et al., 1994; Smelror et al., 1994, 1998, 2001). Both *Spekk* and *Hekkingen* formations consist of immature to marginally mature sediments with high TOC contents relative to average shale (e.g. Wedepohl, 1971, 1991). A significant TOC decrease towards the top of both formations, which is

most severe during the Berriasian, is owing to increased bottom water oxygenation that was likely caused by a rapid sea-level rise (e.g. Mutterlose et al., 2003; Langrock et al., in press).

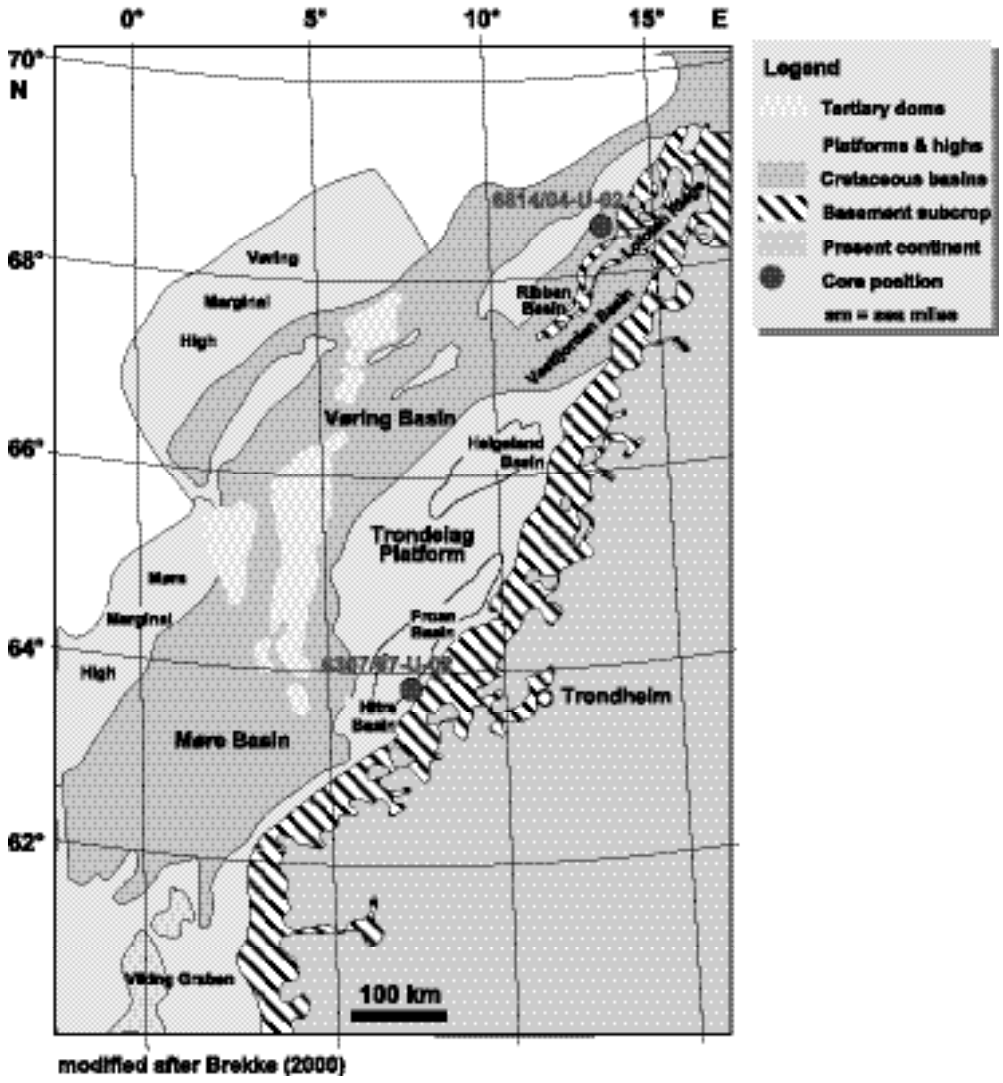

Fig. 4-1 Geographic section of the modern shelf region off mid-Norway, including principal sedimentary units and positions of drilling holes (modified after Brekke, 2000).

Variations within the formations are linked to 40-ky and 100-ky orbital-forced climate cycles (e.g. Swientek and Ricken, 2001; Swientek, 2002; Mutterlose et al., 2003) and are to some extent superimposed on local effects, such as silt dilution and increased primary production.

Paleogeographic turning points caused by either transgression or regression are favorable for the deposition of organic carbon-rich bituminous rock sequences (e.g. Bitterli, 1963), especially during the initial stage of such episodes (e.g. Sheridan, 1987). Collected research data suggest

that most organic carbon accumulates in transitional (brackish) or alternating marine/freshwater regimes. Accumulation of particulate organic matter derived from terrestrial sources is subject to fractionation by wind or water, so that larger particles are usually deposited closer to the shore, e.g. in the estuaries.

Small-sized particulate organic matter (< 5µm) is hydrodynamically similar to the clay mineral fraction, which is highly capable to adsorb dissolved organic carbon (DOC, < 0.8 to 0.4 µm) and metal ions to form organo-metal complexes. The conversion from the dissolved into the particulate form (by reasons of energy) is often attributed to changing water chemistry within the marine/freshwater transition zone and is especially important in view of petroleum source rock formation (e.g. Calvert and Pedersen, 1992; Meyers, 1997). The relationship between hydrocarbon source rocks and their depositional environment has been reported from several locations (e.g. Boussafir and Lallier-Vergès, 1997; Schulz et al., 2002). Two principal models for the causes of vast organic carbon accumulation have been under controversial discussion during the past three decades: (1) ocean wide episodes of “stagnation” in restricted stratified basin similar to the Black Sea, and (2) an increased primary production which causes oxygen minimum zones that impinge on the sea floor and thereby limit the remineralization of organic matter on the sea-floor [e.g. Pedersen and Calvert, 1990, Caplan and Bustin, 1999; Saelen et al., 2000; Nijenhuis et al., 2001; Röhl et al., 2001]. An increased supply of terrigenous organic matter may also be an important mechanism for the accumulation of organic carbon-rich sediments in the marine realm [e.g. Stein et al., 1986]. The high northern paleolatitudes also received attention by scientists because most common information about formation of organic carbon-rich sediments was obtained largely from lower paleolatitudes, e.g. the Mid-Cretaceous Atlantic Ocean, but also the Tertiary Indian Ocean (e.g. Schlanger and Jenkyns, 1976; Stein et al., 1986; Brumsack and Thurow, 1987; Arthur et al., 1990; Bralower et al., 1994; Bralower and Thierstein, 1984, 1987; Siesser, 1995; Herrle et al., 2003).

The primary objective of this paper is concerned with the origin of the organic carbon that has generated the source rock potential found in these immature sediments. Once the sources of the associated organic matter are determined from a detailed microscopic analysis, mass accumulation rates of organic carbon and paleoproductivities are calculated and interpreted in relation to the depositional environment.

4.2. Data and procedures applied

Material was collected from two sediment cores drilled offshore mid-Norway during a prospective campaign executed by Sintef Petroleum Research (former IKU) in the late 1980´s (Fig. 4-1) (e.g. Fjerdingstad et al., 1985; Århus et al., 1987; Skarbø et al., 1988; Bugge et al., 1989; Hansen et al., 1991). Core 6307/07-U-02 was taken in the southern part of the Hitra Basin (off Smøla island, 63°27´54´´ N and 07°14´44´´ E) in a water depth of 290 m. Core 6814/04-U-02 was taken approximately 354 nautical miles (655 km) further to the NNE in the northern part of the Ribban Basin (near the Lofoten Islands, 68°09´45´´ N and 14°09´47´´ E) in a water depth of 233 m. Below a Quaternary cover, the cores immediately penetrate 104.80 m and 191.25 m, respectively, of shallow, WNW dipping Mesozoic strata that encompass the Kimmeridgian-Valanginian and Volgian-Barremian interval (Fig. 4-2). The cores were sampled in irregular intervals of 1.5 – 2.0 meters, depending on the physical condition and the availability of the material, resulting in a time resolution of about 120 to 350 ky (cf. Mutterlose et al., 2003). Kerogen typing, determination of source rock generative potential and organic matter (OM) maturity were conducted according to Espitalié et al. (1977, 1985) and Peters (1986) using a Rock-Eval II (*plus S3 unit*). The hydrogen index (HI) was calculated from the amount of pyrolysable hydrocarbons (S2 value) based on the TOC content, and the oxygen index (OI) was calculated from the amount of associated carbon dioxide (S3 value) based on the TOC content. Indices were used in a HI/OI diagram to estimate kerogen types (I – IV), their potential sources and thermal maturity [cf. Espitalié et al, 1977; Peters, 1986].

The determination of the particulate organic matter (POM) was performed by means of maceral analysis. For this purpose 40 whole rock samples were collected from both sediment cores. The preparation of kerogen isolates was not necessary since the organic carbon content of the samples was relatively high (1 – 7 wt %). The small blocks of rock (3 – 4 cm^3) were orientated perpendicular to the bedding and fixed by a cold-setting epoxy-resin. After hardening they were successively ground and polished with diamond paste in multiple stages on an automatic unit to obtain optimal reflection properties. The macerals were identified by point-counting with a 25-point ocular grid using a Zeiss Axiophot microscope under incident and fluorescence light (395 – 440 nm). For statistical accuracy at least 200 macerals were counted in each sample. Macerals were distinguished into tree main groups vitrinite, inertinite and liptinite

and were subdivided in subgroups and individual macerals according to the ICCP nomenclature described in Taylor et al. (1998). Vitrinites are cellulose and lignin-rich remains of higher land-plants, e.g. tissues of leaves or tree bark, and usually produce type II/III to III kerogen (cf. Espitalié et al., 1977; Peters, 1986; Horsfield et al., 1987). Inertinites may have similar sources as vitrinites but they have experienced distinct oxidative alteration, e.g. by wildfires or acidic environments. This results in a depletion of hydrogen and nitrogen and an enrichment of oxygen and carbon compounds which make them virtually inert to maturation processes (e.g. type IV kerogen during Rock-Eval pyrolysis). Liptinite is a collective term for all terrestrial and marine/aquatic organic matter which is rich in lipids and proteins, and that is characterized by distinct fluorescence properties. Terrestrial liptinites are derived from land-plant precursors (e.g. resins, waxes, cuticles, spores and pollen). Hence, for paleoenvironmental reconstruction and source rock characterization it is also important to discriminate the origin of the liptinite fraction of the organic matter.

4.3. Results

4.3.1. Base geochemical data

Core 6307/07-U-02 shows TOC contents between 0.1 and 7.0 wt. % that continuously decrease from the early Volgian to the late Ryazanian (Fig. 4-2). The decrease is particularly rapid through the Ryazanian. Except a few fluctuations in the early Valanginian, the uppermost 20 meters of core 6307/07-U-02 are virtually barren of organic carbon. HI values show high variability between 200 to 600 [mg HC/g TOC] from the early Volgian to the late Ryazanian. In the Valanginian values drop below 200 [mg HC/g TOC] and reach zero in the Hauterivian. TOC contents of core 6814/04-U-02 range from 0.1 to 4.8 wt. % and decrease similar to those in core 6307/07-U-02 (Fig. 4-2). Fluctuations in the early Valanginian are also comparable to core 6307/07-U-02, and the succeeding Hauterivian is virtually barren of organic carbon. HI values range from 200 to 400 [mg HC/g TOC] in the early Volgian and from 100 to 200 in the

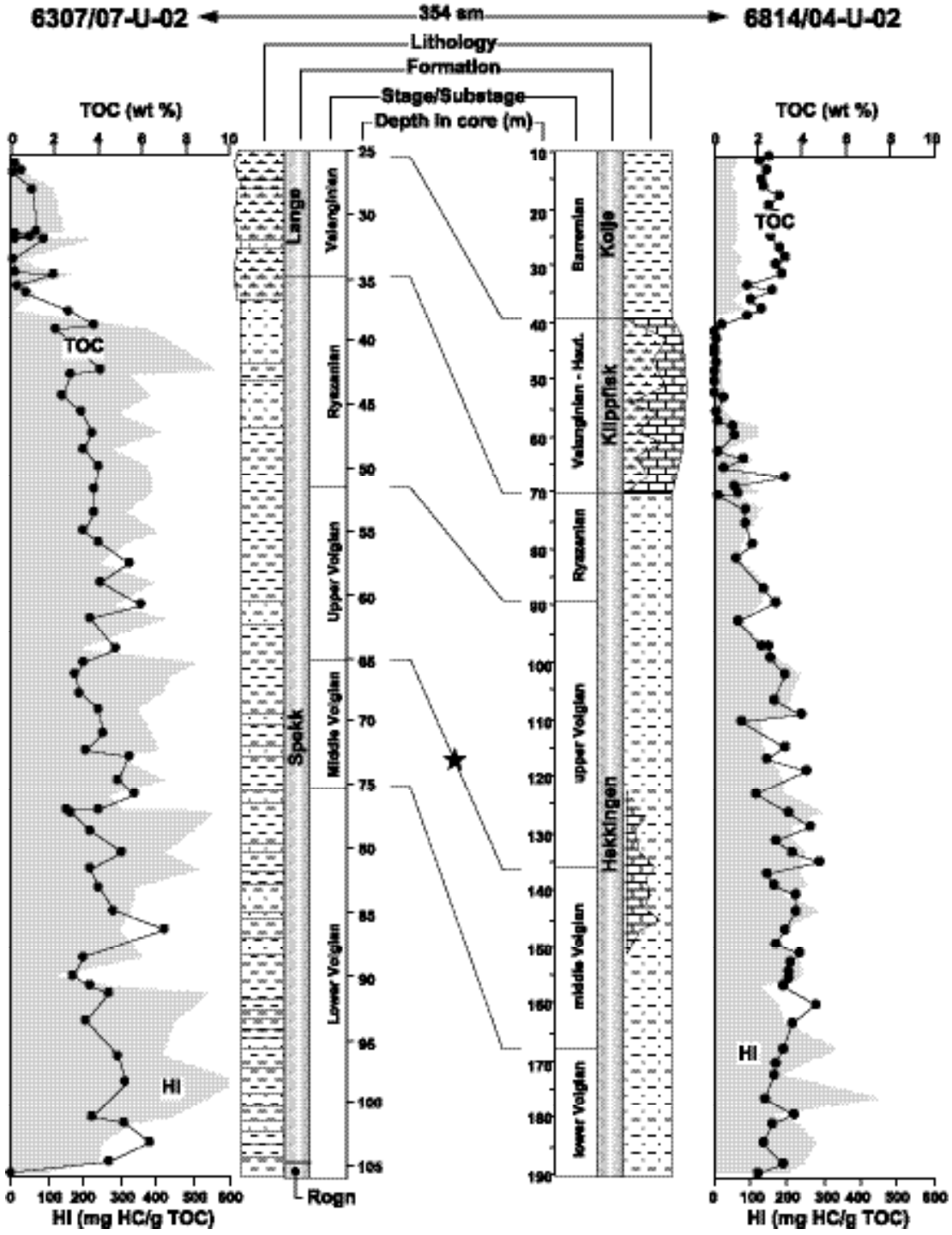

Fig. 4-2 Organic carbon content and Rock-Eval hydrogen index values of core 6307/07-U-02 and 6814/04-U-02. Essential differences were stressed-out by using identical scales. Time correlation, formations and lithology were collected from Brekke et al. (1999), Hansen et al. (1991), Smelror et al. (1994, 1998), Hardenbol et al. (1998), and Mutterlose et al. (2003).

Ryazanian. The Valanginian is marked by values below 100 [mg HC/g TOC], whereas no values can be calculated in the Hauterivian because the TOC is too low.

4.3.2. Organic matter composition

The maceral composition of particulate organic matter (POM) was characterized on whole rock samples following largely the ICCP nomenclature described in Taylor et al. (1998) with the exception of funginite, which was introduced by Lyons (2000). A general overview of the organic matter composition is presented in Figure 4-3 and the total inventory, sources and optical properties observed are summarized in Table 4-1. In total, three maceral groups (vitrinite, inertinite, liptinite), twelve individual macerals and one microlithotype were identified under reflected white light and fluorescence light (picture gallery of microscopic photographs is available at www.pangaea.de/data).

Maceral Group	Maceral & Microlithotype*		Source	Reflected light	Fluorescence color	Form
Vitrinite	Telinite		woody tissues, primary	dark grey/medium gray	none	cellular/subrounded
	Vitrodetrinite		woody tissues, reworked	medium grey	none	cellular, brittle
Inertinite	Fusinite		woody tissues, charred	light grey	none	cellular, brittle
	Semifusinite		woody tissues, charred	grey (bronze hue)	none	cellular, brittle
	Funginite		fungal bodies	light grey/grey	none	cellular
	Inertodetrinite		woody tissues, charred	light grey/grey	none	brittle
	Semifusite*/Fusite*		coalified stems, twigs > 1mm	brownish grey/white	none	sub-cellular layers
Liptinite	terrigenous	Sporinite	land-plant spores	dull brown/translucent	yellow/orange/brown	whole spores
		Cutinite	land-plant cuticles	dull brown/translucent	yellow/orange/brown	
		Resinite	waxes, oils, fats, resins	dull brown/translucent	orange	amorphous
	marine-aquatic	Telalginite	freshwater/marine algae	dull brown/translucent	yellow	cellular, fragmented
		Lamalginite	freshwater/marine algae	dull brown/translucent	yellow/brown	thin bands
		Dinocysts	Dinoflaggelates	dull	green/yellow/brown	cellular, fragmented
	Liptodetrinite		marine-aquatic, various	dull	green/yellow	various disrupted

Table 4-1 General inventory of macerals, including their sources and optical properties, observed in the sediments. In total, three maceral groups (vitrinite, inertinite, liptinite), twelve individual macerals and one microlithotype were identified under reflected white light and fluorescence light.

Macerals of the vitrinite group are identified as dark gray to medium gray telinite (≥ 10 µm) and more light-colored vitrodetrinite (≤ 10 µm). None of the vitrinites show any fluorescence. Their shapes vary from sub-rounded and sub-angular particles to excellently preserved cellular tissues, i.e. from land-plant leaves or bark. Most telinites are between 20 and 100 µm in size, some exceed 200 µm, and a few cellular individuals reach more than 500 µm with a length/width ratio of up to 10:1. Particularly, in the late Volgian sequence from the Ribban Basin telinite smaller than about 40 µm tend to be more rounded and of lower maturity, whereas larger macerals tend to be more angular, structural better preserved and of higher maturity. Open cell-fillings consisting of admixtures of collinite (cf. Taylor et al., 1998) and mineral matter occur rarely and were not quantified. It was also observed that larger telinites (100 – 300 µm) with lower reflectivity are associated with much smaller macerals (10 – 50 µm) of the inertinite group and vice versa.

Macerals of the inertinite group are present as fusinite, semifusinite, funginite, and inertodetrinite. Although semifusinite is almost absent in core 6307/07-U-02, the macerals of the inertinite group have a significantly higher abundance (up to 20 %) compared to the core from the Ribban Basin (≤ 5 % of the POM) (Fig. 4-3). Generally, particles with higher reflectance and maturity are much more angular and cellular compared to other woody particles of lower maturity, i.e. telinite. Fusinite and semifusinite generally show very well preserved cell structures with curved edges, i.e. bogen structure and sieve-structure, and a broad spectrum of reflectivity. A combination of high structural integrity and various stages of fusinitization suggest that incomplete charring by wildfires (i.e. pyrofusinites) has caused maturity rather than by coalification during diagenesis (i.e. rank fusinites) (Taylor et al., 1998).

Some pyrofusinites look like hair slides, almost white in reflected light and up to 100 µm in length. Semifusinites show optical reflection properties between those of vitrinite and fusinite, and they appear with a hue of bronze. These well preserved fragments often appear in clusters, or in partly fractured and shattered cellular bodies, but also as single particles up to 200 µm in size. Some medium-sized (50 to 80 µm) macerals are also found with a rectangular shape, lacking any cellular structure. Semifusinites is also often observed as scleres with sharp edges and spikes, forming a heap of ruins (“Trümmerfeld”) that sometimes exceeds 200 µm in size. The shape of such heaps suggests that the pieces have broken apart from larger plant tissues in situ, hence, after their deposition as a result of compaction.

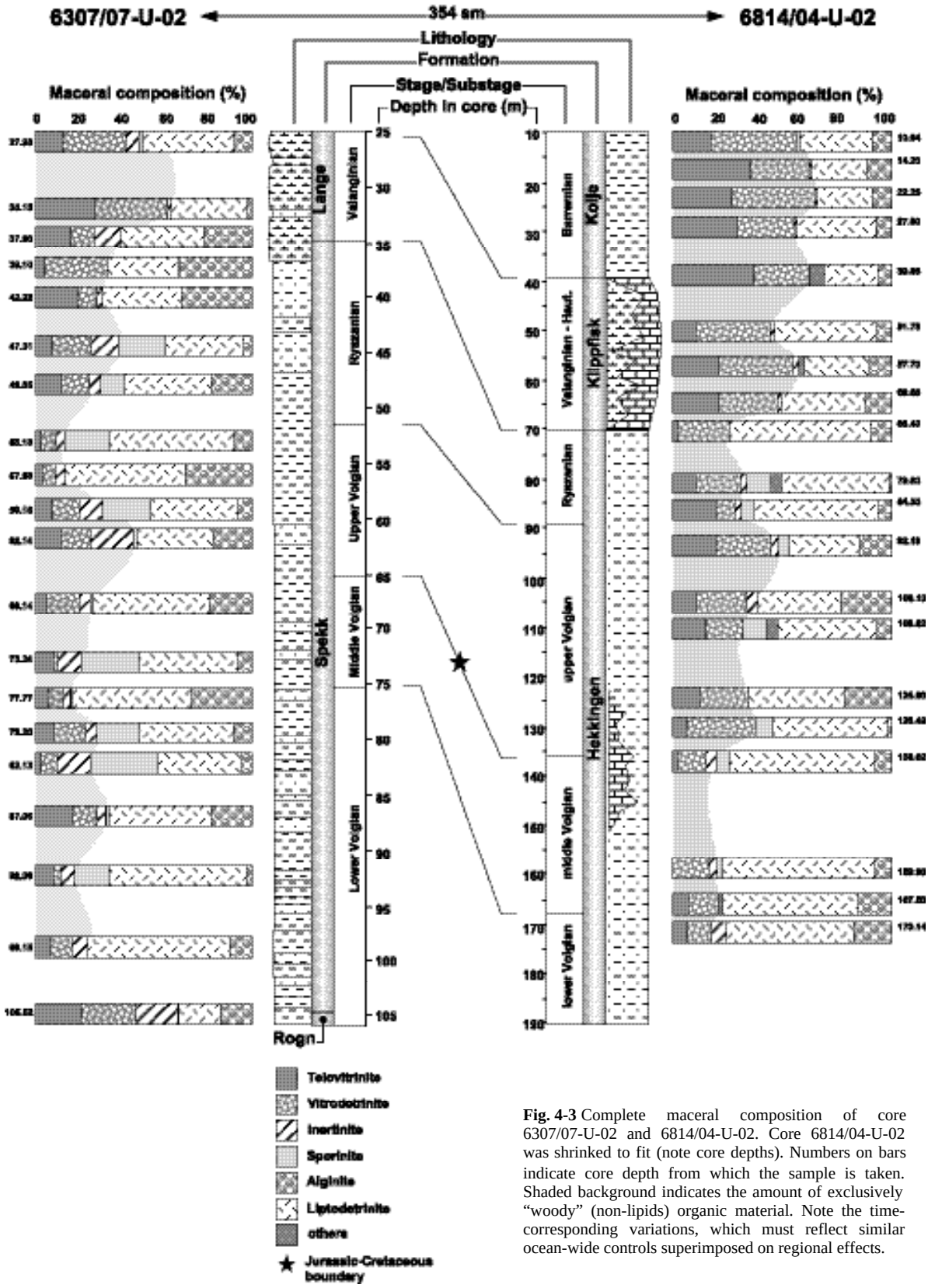

Fig. 4-3 Complete maceral composition of core 6307/07-U-02 and 6814/04-U-02. Core 6814/04-U-02 was shrinked to fit (note core depths). Numbers on bars indicate core depth from which the sample is taken. Shaded background indicates the amount of exclusively "woody" (non-lipids) organic material. Note the time-corresponding variations, which must reflect similar ocean-wide controls superimposed on regional effects.

Funginite, formerly addressed as sclerotinite, is rarely found and consists of very well preserved opaque cellular bodies (from sclerotia) with regular cell structures and high reflectivity (cf. Lyons, 2000; Langrock et al., 2003). There is a spectacular vascular bundle of 2 mm length and 0.2 mm width showing extremely well preserved cell structures and high reflectivity. It consists of different compressed layers of fusinite and likely reflects a part of a *fusite* microlithotype rather than a single plant tissue.

Macerals of the liptinite group must be distinguished into terrigenous and marine-aquatic liptinite. Sporinite is the most dominant and unmistakable terrigenous maceral and occurs in different morphologic types of microspores, ranging from about 10 to 200 µm in size. Individuals usually appear as collapsed spheres with relatively thick cell walls and single- or multi-layered exines. Larger forms with typical transected star ledges are rarely observed, whereas fractured exines of smaller forms are more common. Under fluorescence light sporinite shows a variety of colors from clear yellow to brown, reflecting different stages of biodegradation. Similar to inertinite the total amount of sporinite is much higher in the southerly core (max. 35 % POM) (see Fig. 4-3). Cutinite and resinite are abnormally rare in both cores and have been identified in only a few cases. Usually, cutinite originates from cuticular layers and cuticles and is probably the most resistant material produced by common land-plants (e.g. Taylor et al., 1998). Owing to its scarcity it was not usable for quantification, but this may have important paleoclimatic and paleogeographic implications. A determination between terpene resinite (originated from resins), or lipid resinite (originated from fats) was not successful. Generally, terrigenous liptinites (especially sporinite) become abruptly rare and then absent in the upper parts of the *Spekk* and *Hekkingen* formations, probably reflecting the increasing distance to the paleo-shore (e.g. Littke et al., 1997; Langrock et al., 2003; Mutterlose et al., 2003). The origin of marine liptinites is much more difficult to determine and has been subdivided into alginite (telalginite and lamalginite) and liptodetrinite. Visible entities of large colonial or thick-walled unicellular algae with a distinctive structure are termed telalginite. Four different types of telalginite were identified (in order of abundance): dinoflagellates (cysts), *Pila, Tasmanites,* and *Pediastrum.* Dinoflagellate cysts occur numerously throughout both cores in nearly equal quantities, except for elevated abundance in the upper *Spekk* Formation. These organic remnants of algae appear as chorate cysts with different types of single and branched processes and radiating spines. At least 5 different morphotypes were identified from 10 to 80 µm in diameter. The largest individuals

show most severe marks of degradation, both physical and biochemical. The smallest individuals of less than 20 µm in size are more likely acritarchs rather than dinocysts because distinctive taxonomic indications are missing, e.g. the archaeopyle, and acritarchs usually develop smaller individuals (e.g. Williams, 1980). One species is most common in both cores and shows a spectacular bright green fluorescence color, reflecting their excellent preservation in physical and biochemical views. These individuals are about 10 µm in size with short single processes relative to their body and probably belong to the *Micrhystridium* lineage (e.g. Combaz, 1980). Algae of *Pila* type are usually compared to the modern *Botryococcus braunii*, which reproduce exclusively in freshwater habitats. These algae were observed occasionally but are generally more common in the southerly core. Degradation is sometimes at an advanced level but the original colonial structure can be distinguished in most cases. *Tasmanites* algae are compared to the modern analogue *Pachysphaera pelagica* and were observed at various depths in both cores, emitting an intensive yellow fluorescence color. The physical preservation is generally much better than that of *Pila* colonies, because *Tasmanites* is unicellular and has a more inflexible cell wall. They appear as flat thick-walled discs perpendicular to the bedding and reach 120 µm in length that may be about 80 µm in original diameter. Their original spherical form and characteristic numerous pore-canals, which penetrate the outer cell wall and leave small dimples on its surface, can be clearly identified when observed under reflected white light. In sediments deposited under more oxygenated conditions, particularly in the Lange and Klippfisk formations, the formation of idiomorphic pyrite within some telalginites is a common process and reflects anoxic micro-environments below the sediment surface. Lamalginite, on the other hand, is less common in the sediments and appears as thin-walled filamentous algae of weak to medium yellow fluorescence color and a distinctive lamellar form parallel to the bedding.

Most macerals of the liptinite group are detrital (30 to 70 %) (Fig. 4-3), which is usually very difficult to address to a discrete biological source. However, the majority of the liptodetrinite appears to be of marine-aquatic origin that is a crucial point, particularly when calculating paleoproductivities. Our observations revealed that terrigenous liptinites derived from the Norwegian coastland, i.e. dominantly spores, are much more resistant to physical disintegration than marine-aquatic organisms. The shape of most liptodetrinite macerals suggests that they have been derived from the fragile parts of marine organisms, such as most dinocysts and other algae. Supporting this, a large amount of liptodetrinite, though heavily crushed into pieces, has still

higher fluorescence colors (shorter wavelength) than most intact terrigenous liptinite. Since the wavelength of fluorescing particles becomes longer with progressing biodegradation, i.e. more red colors when observed under the microscope, a land-plant source for liptodetrinite in our sediments is very unlikely. It has therefore in major parts been counted to the marine-aquatic organic matter.

4.3.3. Accumulation rates of organic carbon

It is difficult to interpret TOC data, particularly in coastal environments, because changes in the percent values of TOC may result from both organic and sedimentological changes (e.g. Stein et al., 1986). Therefore, we calculated mass accumulation rates of organic carbon to reflect the authentic organic carbon received by the sediment surface in units of mass per area and time, so avoiding effects of clastic dilution (cf. Van Andel, 1975; Thiede et al., 1982).

Period	**Linear sedimentation rate**		
	(cm per 1000 years)		
Stage/substage	biostratigraphic		astronomical
	6307/07-U-02	6814/04-U-02	
Barremian	-	0,8	-
Hauterivian	0,3	0,3	-
Valanginian	0,3	0,3*	0,4*
Ryazanian	0,4	0,8	-
Late Volgian	0,5	1,5*	1,6*
Middle Volgian	0,3	0,8	-
Early Volgian	0,8**	0,6	0,8**

* peaks from spectral analysis investigated in core 6814/04-U-02 (after Swientek, 2002)

** peaks from spectral analysis investigated in core 6307/07-U-02 (after Swientek, 2002)

Table 4-2 Comparison between biostratigraphic and astronomical linear sedimentation rates (LSR) on the left and cyclicity-tuned LSR used in this paper (cf. Swientek and Ricken, 2001; Mutterlose et al., 2003).

Physical properties of the sediment and stratigraphic control are imperative for calculating mass accumulation rates. Whereas bulk density and porosity are easily available, biostratigraphic control on late Mesozoic black shale sequences is almost always a problem, particularly when dealing with very low sedimentation rates. Time control for the investigated cores was obtained

largely from lithostratigraphic, palynological, and biostratigraphic studies [e.g. Skarbø et al., 1988; Hansen et al., 1991; Mutterlose et al., 2003; Smelror, 1994; Smelror et al., 1998, 2001; Vigran et al., 1998; Worsley et al., 1988]. Using the time scales of Hardenbol et al. (1998) the resulting linear sedimentation rates (LSR) are supported by a good correlation between biostratigraphic and astronomical dates (e.g. Berger et al., 1992; Oschmann, 1995; Swientek and Ricken, 2001), which is presented in Table 4-2. It has to be considered, however, that pitfalls in the calculation of LSR may be caused by hiatuses in the Valanginian and Hauterivian, especially when the duration is uncertain. With the amount of marine organic matter obtained from maceral composition by kerogen microscopy, it was possible to calculate mass accumulation rates of marine organic carbon and eventually estimating paleoproductivities (see below). Mass accumulation rates of total organic carbon (MARTOC) in core 6307/07-U-02 show values that range from 60 to 80 mg/cm^2/ka in the lower Volgian and drop to ≥ 40 mg/cm^2/ka in the upper Volgian. From here values decrease upwards to ≥ 20 mg/cm^2/ka in the Ryazanian (Berriasian) and lower Valanginian (Fig. 4-4).

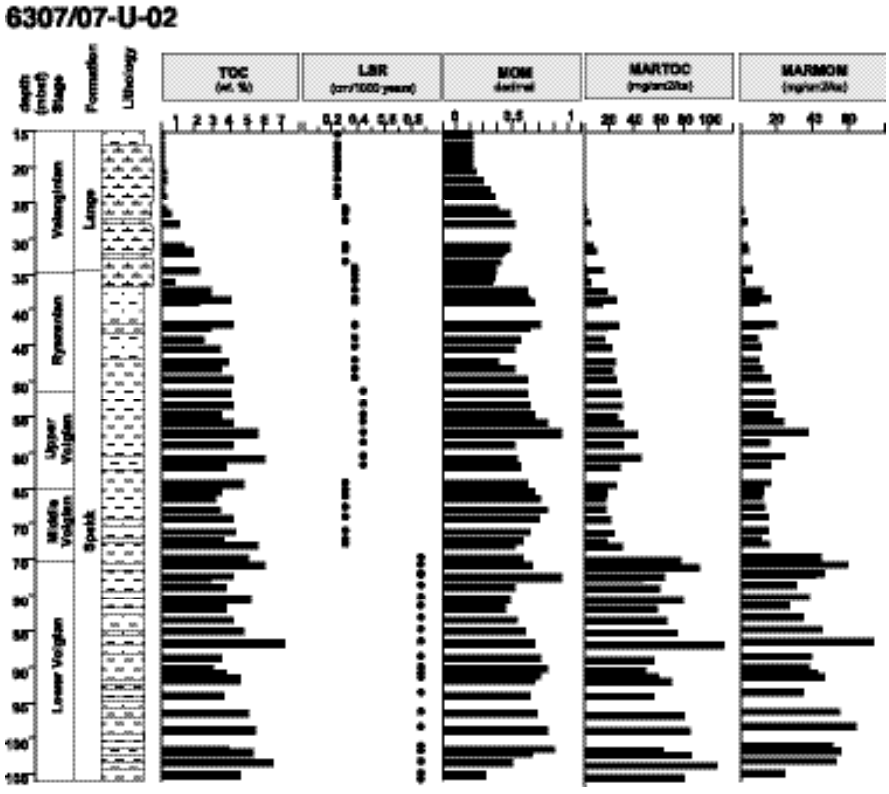

Fig. 4-4 Organic carbon content (Langrock et al., in press), corrected linear sedimentation rates (Mutterlose et al., 2003), marine organic matter (MOM) content (this paper), and mass accumulation rates of total organic carbon (MARTOC) and marine organic carbon (MARMOM) for core 6307/07-U-02.

The decrease towards the top of the core is a reflection of the TOC content and accelerated by the decreasing sedimentation rates. Based on the amount of marine organic matter (MOM) obtained from maceral analysis, accumulation rates of marine organic carbon (MARMOM) show a corresponding decrease from about 60 mg/cm^2/ka to ≥ 10 mg/cm^2/ka. Mass accumulation rates of total organic carbon (MARTOC) in core 6814/04-U-02 show values that increase from about 40 mg/cm^2/ka in the lower Volgian to 100 - 150 mg/cm^2/ka in the upper Volgian (Fig. 4-5). The decrease is also a reflection of the TOC content, resulting in a rapid decrease of MARTOC from ≥ 40 mg/cm^2/ka in the Ryazanian to ≥ 10 mg/cm^2/ka in the Valanginian and Hauterivian. Values from 40 to 60 mg/cm^2/ka are dominant throughout the succeeding Barremian. Based on the amount of marine organic matter (MOM) obtained from maceral analysis, accumulation rates of marine organic carbon (MARMOM) show corresponding values from about 20 to 80 mg/cm^2/ka with maximum values in the lower part of the upper Volgian.

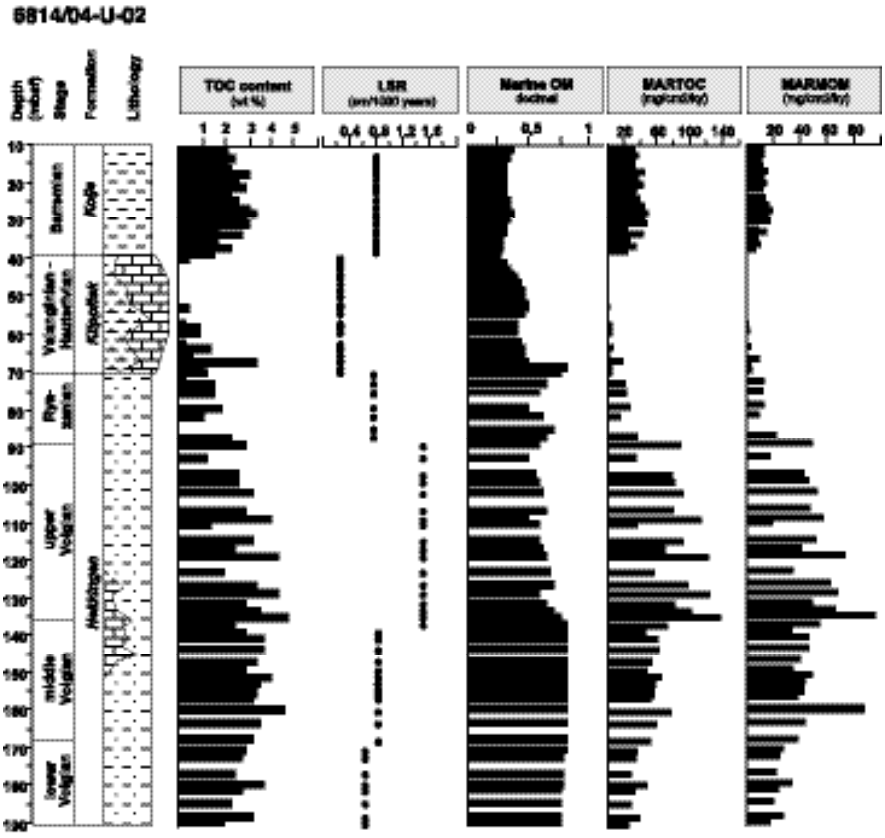

Fig. 4-5 Organic carbon content (Langrock et al., in press), corrected linear sedimentation rates (Mutterlose et al., 2003), marine organic matter (MOM) content (this paper), and mass accumulation rates of total organic carbon (MARTOC) and marine organic carbon (MARMOM) for core 6814/04-U-02.

4.4. Discussion

4.4.1. Organic facies types

The concept of organic facies types has once been develloped by coal petrographers. They found that distinct coal macerals were generally deposited in distinct groups under similar chemical and physical conditions, and they defined organic facies types with special emphasis on its application in the oil industry (e.g. Jones, 1987; Taylor et al., 1998). Jones (1987) distinguished seven organic facies types (Table 4-3) only by the dominant type of organic matter, the atomic H/C ratio (at vitrinite reflectance R_0 ± 0.5 %) and HI and OI values obtained from Rock-Eval pyrolysis. The organic facies types reflect a decrease in the marine/aquatic and an increase in terrestrial/oxidized organic fraction of the sediment, documenting a successive reduction of the petroleum generative potential.

Organic facies	H/C (at R0 ±0.5 %)	Hydrogen Index (mg HC/g TOC)	Oxygen Index (mg CO_2/g TOC)	Dominant organic matter
A	≥ 1.45	≥ 850	≤ 30	algal, amorphous
AB	1.35 - 1.45	650 - 850	20 - 50	amorphous, minor terrestrial
B	1.15 - 1.35	400 - 650	30 - 80	amorphous, common terrestrial
BC	0.95 - 1.15	250 - 400	40 - 80	mixed, some oxidation
C	0.75 - 0.95	125 - 250	50 - 150	terrestrial, some oxidation
CD	0.60 - 0.75	50 - 125	40 - 150	oxidized, reworked
D	≤ 0.60	≤ 50	20 - 200	highly oxidized, reworked

Table 4-3 Classification scheme of organic facies types after Jones (1987)

According to the differentiation scheme of Jones (1987) shown in Table 4-3, we observed organic facies B to D in both cores, whereas organic facies A and AB are absent (Fig. 4-6, Fig. 4-7). Highest organic facies (B and BC) were found in the lower third of the cores and correspond to highest TOC and HI values and highest abundance of lipid-rich organic matter (cf. Fig. 4-3). In core 6307/07-U-02 organic facies BC is present throughout the lower, middle and upper Volgian and in the lower Berriasian (Fig. 4-6).

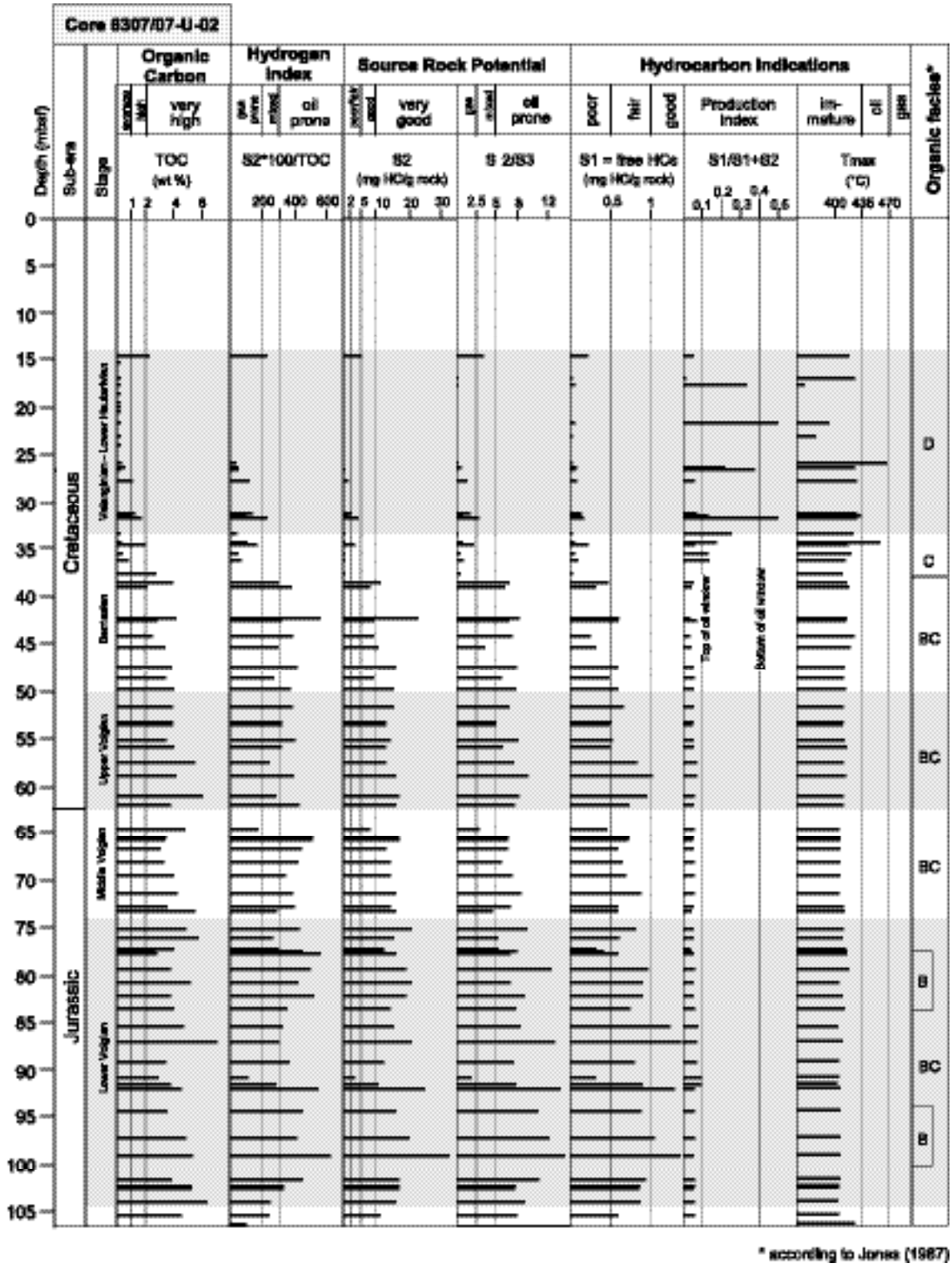

Fig. 4-6 Organic carbon, hydrogen index, source rock potential, and organic facies (after Jones, 1987) for core 6307/07-U-02. Note that production index and T_{MAX} are abnormally high in sequences of extremely low TOC that do neither reflect hydrocarbon generation nor passed maturity.

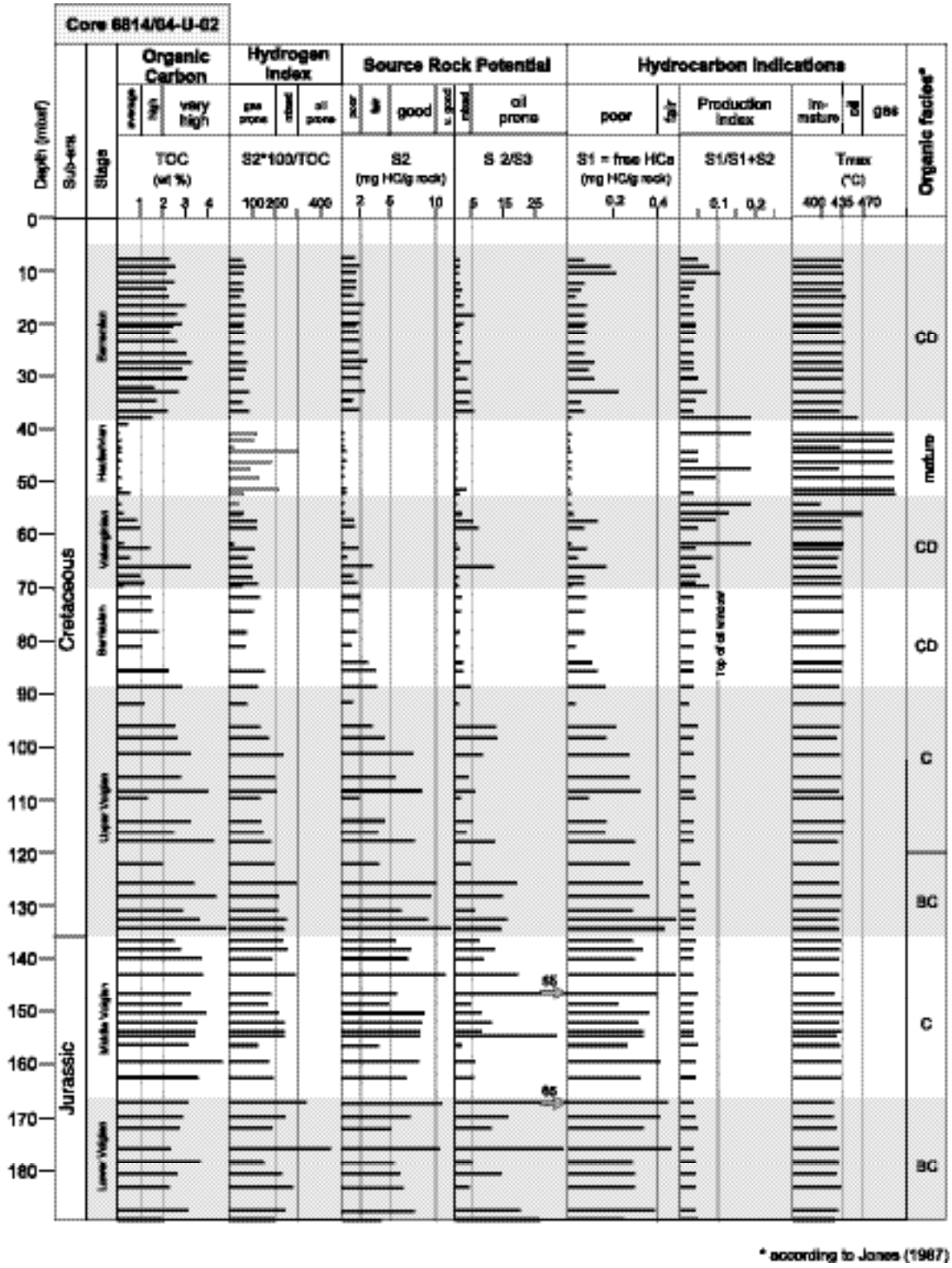

Fig. 4-7 Organic carbon, hydrogen index, source rock potential, and organic facies (after Jones, 1987) for core 6814/04-U-02. Note that production index and T_{MAX} may be abnormally high in sequences of extremely low TOC that do neither reflect hydrocarbon generation nor passed maturity.

Only two distinct periods in the lower Volgian reveal organic facies B. In core 6814/04-U-02 (Fig. 4-7) the same period of time is characterized by a less constant facies distribution, as organic facies BC and C (lower and middle Volgian) is succeeded by organic facies C (upper Volgian) and CD (Berriasian). A common feature of both cores is that the Klippfisk and Lange formations of the Valanginian and especially the Hauterivian are dominated by organic facies CD and D.

4.4.2. Source rock potential and paleoenvironment

The *Spekk* Formation of core 6307/07-U-02 has crucial prerequisites to be a black-shale in the sense of Tissot and Welte (1984) because the sediments are rich in organic carbon compared to average shale (Fig. 4-6) (Wedepol, 1971, 1991). High preservation of lipid-rich organic matter is reflected by HI values from 300 to 600 [mg HC/g TOC] providing a very good source rock potential for oil. Indications of free hydrocarbons ("oil shows") reflected by the S1 value are good in the lower parts of the *Spekk* Formation and decrease towards the top similar to the source rock potential. Production index (PI) and T_{MAX} values indicate that the organic matter is immature (< 435°C) and has not yet reached the top of the oil-window (PI < 0.1). Organic carbon content and source rock potential decrease during the upper Berriasian and the Valanginian and reach almost zero during the Hauterivian. Here, the residual amount of organic matter consists of refractory material (inert and almost exclusively terrestrial) as a result of oxidative fractionation. As a consequence, T_{MAX} and PI values rise and give the false evidence of hydrocarbon generation. The previous classification of organic facies (Jones, 1987) coincides with these results and reflects the increasing dominance of highly oxidized and reworked organic matter (refractory OM). Even though the *Hekkingen* Formation consists of organic carbon-rich sediments with TOC values higher than 2 % by weight (Fig. 4-7), average values are lower by about 1 % compared to the *Spekk* Formation (cf. Fig. 4-6). The lower potential for a source rock becomes even more clear considering the HI values, which range only from 100 to 300 [mg HC/g TOC] and indicate a much lesser degree of preservation of lipid-rich OM. As a result, the

sediments have only a good to fair source rock potential for generating oil and mixed oil/gas products.

Similar to core 6307/07-U-02 (cf. Fig. 4-6) the source rock potential becomes subsequently poor and more gas-prone during the Berriasian and Valanginian. Free hydrocarbons (S1 value), i.e. “oil shows”, are much less abundant and may have already been released during late diagenesis. This is most likely due to the pre-mature level of the organic matter as indicated by the T_{MAX} (≈ 435°C) values. The distribution of organic facies types according to Jones (1987) in the *Hekkingen* Formation is a positive reflection of the source rock potential. The subsequent Barremian of core 6814/04-U-02 (Fig. 4-7), which is not documented in core 6307/07-U-02, is a period with much less variations in organic carbon and HI values. Even though the TOC content is very high (> 2 %), the source rock potential is poor for generating mixed oil/gas products because the input and/or preservation of lipid-rich organic matter (HI < 100) and the amount of S2 hydrocarbons are also quite low. Therefore, this sequence has been addressed to organic facies CD.

A high source rock potential (subsequently abbreviated as SRP) is often found in immature sediments relatively rich in organic carbon with a high preservation of lipid-rich organic matter (OM) (e.g. Tissot and Welte, 1984). Such sediments are predominantly found in shallow-marine environments because it provides essential nutrients, high input rates of lipid-rich OM from marine (primary production) and terrestrial sources, and relatively short travel time through the water column. In contrast to many upwelling areas, a significant proportion of lipid-rich organic matter from terrestrial sources, such as sporinite and resinite, may contribute to a high petroleum potential of sediments formed in epicontinental seas and shelf basins. For this reason the exclusively use of organic-geochemical approaches for determining OM sources in near-shore environments may produce contradictory results (e.g. Fahl and Stein, 1999). For adequate quantification the “extracted” information, e.g. obtained from biomarker analysis, is often difficult to interpret without invoking the results of other parameters, such as palynological studies or organic petrography (maceral analysis). The optical determination and quantification of organic matter gives a more clear association between organic particles and their biological sources. Because time-resolution of maceral data is usually low as a result of expansive preparation, a combination of organic-geochemical, inorganic-geochemical and petrographic analysis has been successfully applied in recent works (e.g. Kim et al., 1999; Boucsein, 2000;

Caplan and Bustin, 2001; Wagner, 2002; Langrock et al., 2003, Langrock et al., in press). The most significant macerals obtained from petrographic analysis were compared to the SRP and supported by sedimentological and inorganic-geochemical data illustrated in Figure 4-8 and 4-9.

The L* value is obtained from photospectrometry and returns the lightness of a sediment as a kind of gray value, which is primarily affected by the fossil and mineral assemblages (cf. Swientek, 2002). Swientek (2002) clearly demonstrates that low L* values, especially the dark color of black shales, do not reflect high organic carbon contents but the abundance of pyrite. On the other hand, increased L* values indicate more sandy and/or calcareous intercalation, which may indeed be associated with a reduced (diluted) TOC content. Figures 4-8 and 4-9 display remarkable, relatively invariable L* values with a mean of about 30 % for the entire Volgian and Ryazanian. This reflects the vast abundance of pyrite within the dark-colored, organic-carbon-rich sequences of both cores, but pyrite size distribution has shown that sediments of the Spekk formation were deposited under more anoxic conditions compared to the Hekkingen formation (e.g. Langrock et al., in press). An increase by more than 20 % in the Valanginian-Hauterivian clearly documents the formation of more light-colored carbonates and marls under more open-marine oxic conditions (e.g. Mutterlose et al., 2003). Even though that pyrite formation is favored by the availability of H_2S from anaerobic bacterial utilization of lipid-rich OM, no correlation exists between L* values and the abundance of liptinites.

A more consistent picture can be obtained from the Ti/Al ratio (cf. Lipinski et al., 2003). Almost exclusively derived from the continents, titanium is a heavy metal associated with the SiO_2 (quartz) mineral fraction, whereas aluminum is predominantly found in clay minerals. One way to interpret Ti/Al ratios is that an increasing ratio indicates an increasing proportion of silt and sand. Usually, an increase in mineral grain size indicates an elevated transport energy, which may be associated with higher sedimentation rates. Whether these have positive effects or negative effects (clastic dilution) on the organic carbon accumulation depends largely on the dimension of increase and the general sediment fraction. Since river discharge is climate-controlled by weathering of the hinterland, the ratio may also be increased when the input of Al^{3+} from river discharge is extremely reduced, e.g. during arid climate periods and the input of Ti^{4+} becomes enhanced via (desert-) winds.

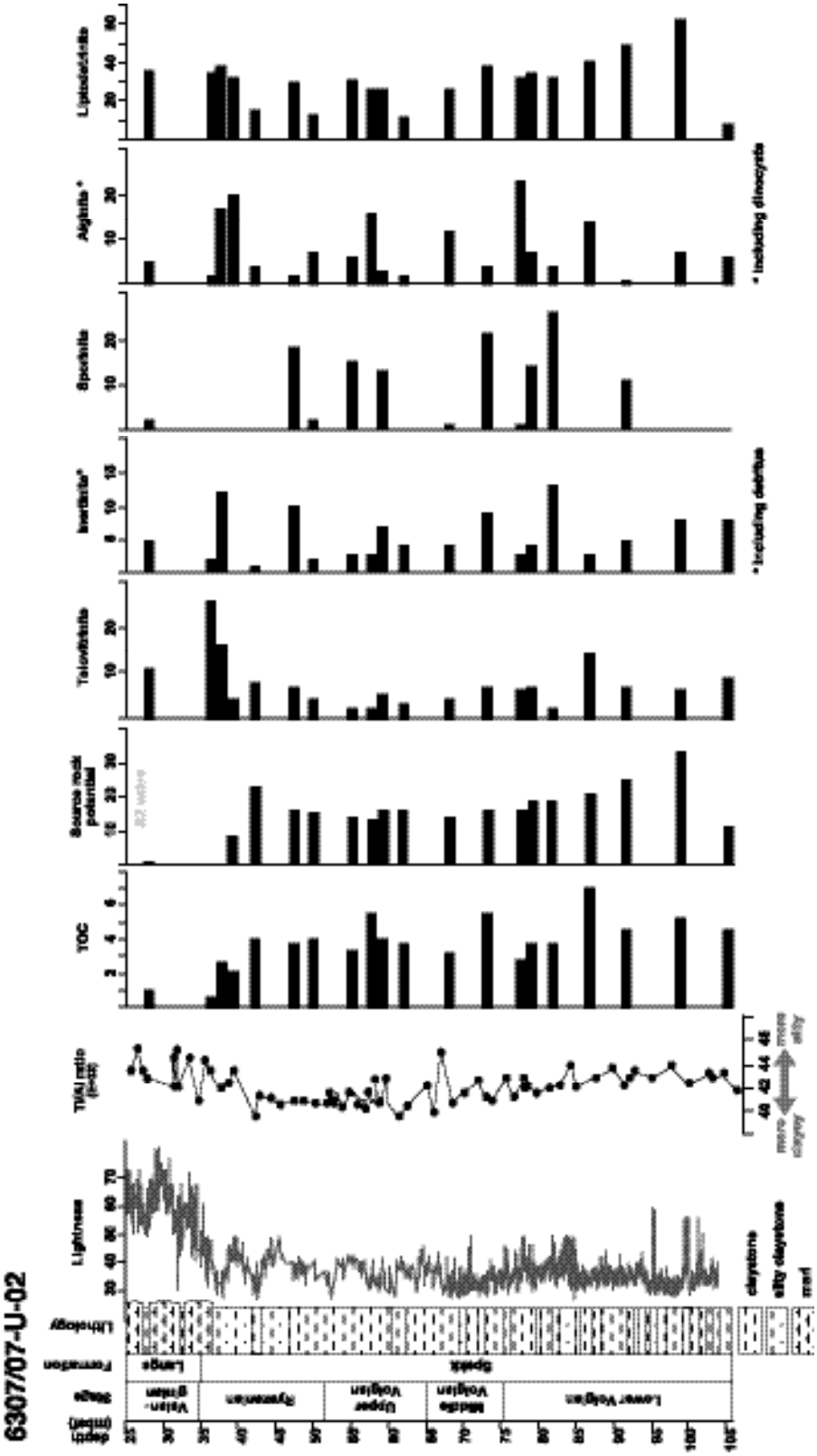

Fig. 4-8 Relationship between source rock potential and selected macerals/maceral groups of core 6307/07-U-02, considering sprectrophotometric L* values (Swientek, 2002) and Ti/Al ratios (cf. Lipinski et al., 2003).

Such a climate has been suggested for the Valanginian-Hauterivian periods (e.g. Podlaha et al., 1998; Mutterlose and Kessels, 2000; Price et al., 2000; Mutterlose et al., 2003), documented in Figures 4-4 and 4-5. Ti/Al ratios are much higher in core 6814/04-U-02 compared to core 6307/07-U-02, indicating that the sediment is generally much more silty (coarser), which likely results in a dilution of the SRP. In the northern core position, low Ti/Al ratios correspond largely to a high TOC content and high SRP (see arrows). This suggests that organic carbon accumulation and preservation of organic matter with elevated SRP is highest in more fine-grained, argillaceous sediments (low Ti/Al ratio). It may therefore be concluded that more coarse-grained, siliceous sediments (high Ti/Al ratio) reflect dilution of the organic carbon content and the SRP. A less obvious relationship between TOC values and low Ti/Al ratios is observed in the southern core position. However, the southern core reveals a good correspondence between high SRP and high Ti/Al ratios on a long-term scale. Hence, it seems that more coarse-grained clastic incursions have a negative influence on the SRP in core 6814/04-U-02 but a rather positive influence in core 6307/07-U-02.

This becomes more evident when the SRP is compared to individual macerals. In core 6307/07-U-02, highest conformity exists between the SRP and the amount of liptodetrinite, whereas no relationship seems apparent to alginite and sporinite (Fig. 4-8). However, organic petrography has shown that most of the liptodetrinite has been produced from the physical breakdown of different algae. Hence, the correlation between SRP and algae is established indirectly over liptodetrinite. The relationship between SRP and more coarse-grained clastic incursions (see above) is now given more sense by the association with lipid-rich detritus. More silty incursions may reflect higher energetic transport and may lead to a higher degree of physical disintegration of algae. The increase of sedimentation rate seems to have no negative effects on the organic carbon content by means of dilution. In the case of core 6814/04-U-02 the SRP is best reflected by the abundance of alginite, which is expected for petroleum source rocks (Fig. 4-9). Based on the above information the SRP and the TOC content are highest during phases of more fine-grained, less energetic clastic sedimentation. This coincides with the results obtained from maceral analysis because the degree of physical disintegration of algae is lower during more “muddy” sedimentation. Hence, the SRP in this area of deposition seems to originate primarily from preservation of non-detrital, primary alginite (including dinocysts). Sporinite and liptodetrinite have different patterns of occurrence, but contributions may not be excluded.

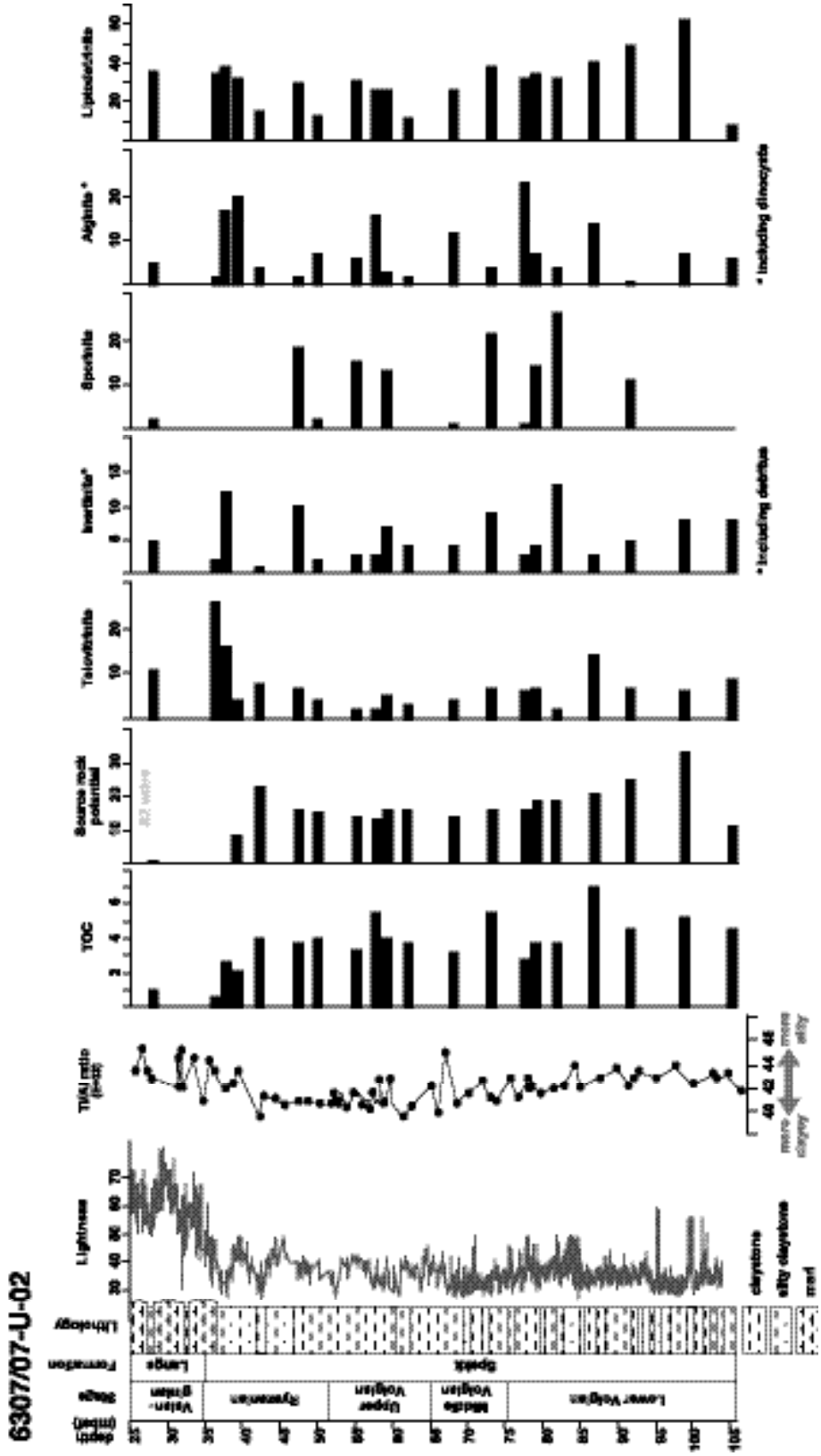

Fig. 4-9 Relationship between source rock potential and selected macerals/maceral groups of core 6814/04-U-02, considering sprectrophotometric L* values (Swientek, 2002) and Ti/Al ratios (cf. Lipinski et al., 2003).

4.4.3. Sporinite paucity

One of the most important observations related to paleoclimatic changes is the striking paucity of sporinite from the middle Ryazanian to the Hauterivian and Barremian in both cores (Fig. 4-8, 4-9; cf. Fig. 4-3). A minor paucity is also apparent during the lowermost Volgian. Sporinite originates from the outer cell walls (exines and perines) of spores and pollen and is composed of sporonin (the fossil term) with the empirical formula $C_{90}H_{85}O_{15}(OH)_4N$ (ash-free "sporin"). This substance is biochemically very resistant and insoluble, but is readily attacked by oxygen under dry conditions, especially in calcareous environments (e.g. Taylor et al., 1998). Keil et al. (1994) found that pollen grains were completely degraded within 10,000 years in the presence of oxygen in the sediment, but were highly preserved for at least 100,000 years under anoxic bottom waters. A change from anoxic/dysoxic, sapropelic environments in the Volgian to more oxic, calcareous environments in the Valanginian-Hauterivian has been documented for the cores investigated by Lipinski et al. (2003) and Langrock et al. (in press). It may therefore be concluded that biochemical preservation of sporinite is much more affected by the redox conditions of the sediment surface than by the conditions of transportation. Particularly in non-upwelling shelf environments with relatively low sedimentation rates, the travel time of particulate matter in the water may be several orders of magnitude shorter than its residence in the upper sediment layers (e.g. Erlenkeuser, 1980).

In general, marine and brackish sediments are characterized by much smaller amounts of sporinite than sediments formed in freshwater environments (e.g. Taylor et al., 1998). The abundance of sporinite and other terrigenous liptinite are therefore often used to indicate proximity to the paleo-coast (e.g. Littke et al., 1997). The relatively high abundance and diversity of sporinite of the studied cores, especially found in the Spekk Formation (Fig. 4-8), suggest that their positions were generally close to the paleo-coast and may reflect a high level of vegetation, which is usually associated with a more warm and humid climate. Although the paucity of sporinite starts very abruptly, it may be correlated to a rapid sea-level rise and a change from a more warm-humid to a more cold-arid climate that commenced in the Ryazanian and reached its maximum in the Valanginian and Hauterivian (e.g. Podlaha et al., 1998; Price et al., 2000; Mutterlose et al., 2003). A similar paucity of sporinite is also reported from the terrestrial Katharina seam of the Ruhr Carboniferous, which is likely a consequence of severe oxidative

degradation by a marine roof succeeding the peat surface. It is therefore suggested that the paucity of sporinite was caused by a combination of (1) increasing distance to the source region, (2) complete oxidation by a rapid marine transgression, and/or (3) a more cool and arid climate.

4.4.4. Depositional environment – stagnation vs. productivity

Calculating the rate in which organic carbon is produced by primary organisms in the photic zone of an ancient ocean is still a puzzling task. A variety of indicators, or proxies, for primary productivity have been suggested, such as accumulation rates of organic carbon, biogenic carbonate, opal flux, and trace elements (e.g. Diester-Haass, 1978; Müller and Suess, 1979; Bralower and Thierstein, 1984; Sarnthein et al., 1987; Stein et al., 1989a, b; Siesser, 1995; Berger and Wefer, 2002; Diester-Haass et al., 2002). The percentage of organic carbon that becomes preserved in the sediment is highly variable and depends on several parameters. In an oxic open-ocean environment with water depths of more than about 1000 meters organic carbon may be so efficiently oxidized that less than 0,1 % may eventually become incorporated in the sediment (e.g. Brummer and Van Eijden, 1992). For this purpose Stein et al. (1986) proposed equation (1) based on Müller and Suess (1979) for calculating paleoproductivity in open-marine oxic environments. For details and limits of use of equation (1) see Stein et al. (1986). On the other hand, sediment data largely obtained from the modern anoxic Black Sea shows that about 2 % of the organic carbon produced in the surface waters becomes preserved in the sediment. This led Bralower and Thierstein (1984) to suggest equation (2) for calculating paleoproductivities in general anoxic environments (e.g. Stein, 1991).

(1) $$PP_{oxic} = 5.31 * (MOM * (WBD - 1.026 * PO/100))^{0.71} * LSR^{0,07} * DEP^{0.45}$$

(2) $$PP_{anoxic} = 50 * C * (WBD - 1.026 * PO/100) * LSR$$

In order to distinguish between oxic and anoxic environments the organic carbon/sedimentation rate relationship is often used (cf. Müller and Suess, 1979; Stein, 1991). However, based on new LSR data presented in Mutterlose et al. (2003) and Swientek (2002) our differentiation has been

improved (Fig. 4-10). Moreover, Lipinski et al. (2003) have demonstrated that redox-sensitive rhenium and molybdenum, in particular the Re/Mo ratio, in the investigated cores may allow to distinguish between anoxic, suboxic, and more oxic water conditions (Fig. 4-11, Fig. 4-12). They showed that depositional conditions in core 6814/04-U-02 were much less anoxic compared to core 6307/07-U-02, which coincides with the results presented in the TOC/SR diagram. It was therefore necessary to calculated PP after both equations (1 and 2) to reveal the most reasonable range of paleoproductivity values according to the conditions in the water column.

In the lower black shale sequence of core 6307/07-U-02 surface water productivity may have reached 20 – 30 gC/m^2/y when using equation (2) (Fig. 4-11). Values are much lower than average productivities estimated for modern coastal environments (50 - 150 gC/m^2/y) (e.g. Pinet, 1992; Tissot and Welte, 1984), anoxic sediments from the Quaternary Sea of Japan (120 – 150 gC/m^2/y) (e.g. Stein, 1991), and even for sediments ≥ 4 wt% TOC from the modern Black Sea (50 – 90 gC/m^2/y) (e.g. Shimkus and Trimonis, 1974; Izdar et al., 1987; Calvert and Vogel, 1987).

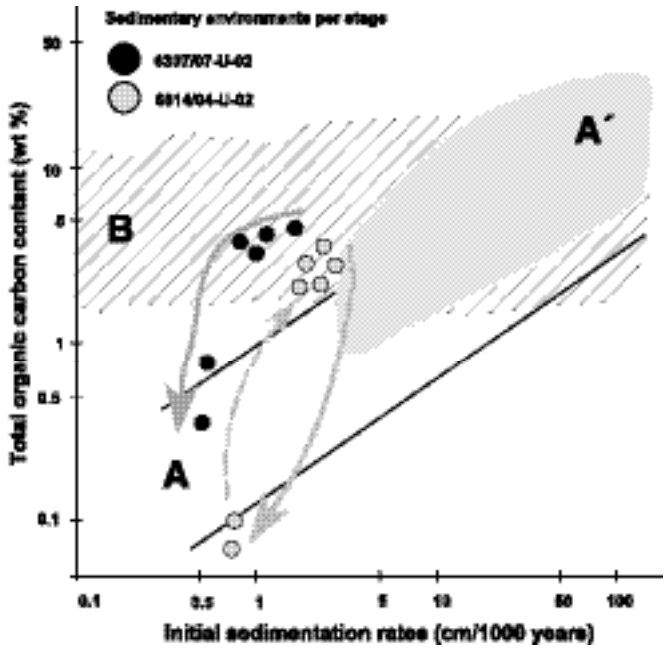

Fig. 4-10 Relationship between (marine) organic carbon content and decompacted sedimentation rates per stage (modified after Stein, 1990, 1991), where different fields of deposition (A=open-marine oxic, A´=high productivity, B=anoxic) are based on results form Recent to Miocene sediments. Each of the circles represent one stage, e.g. the Valanginian. Starting from two different environments the arrows indicate continuous pathways of changes in environmental conditions from the early Volgian to the Hauterivian. Dashed arrow indicates an immediate change of the environment from the Hauterivian to the Barremian in core 6814/04-U-02 back to conditions that once prevailed in the Volgian.

However, our results are much more comparable to the general trend of Mid-Cretaceous black shales (e.g. Bralower and Thierstein, 1987), which show exceptionally low average PP_{anoxic} values from 10 to 100 $gC/m^2/y$.

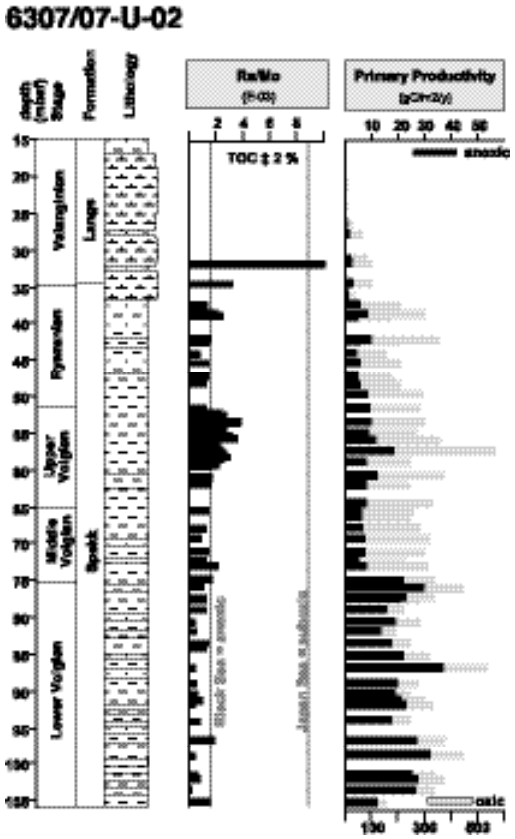

Fig. 4-11 Re/Mo ratios (Lipinski et al., 2003) to discriminate anoxic from dysoxic or oxic environments and paleoproductivity estimates for both oxic (gray) and anoxic (black) conditions for core 6307/07-U-02.

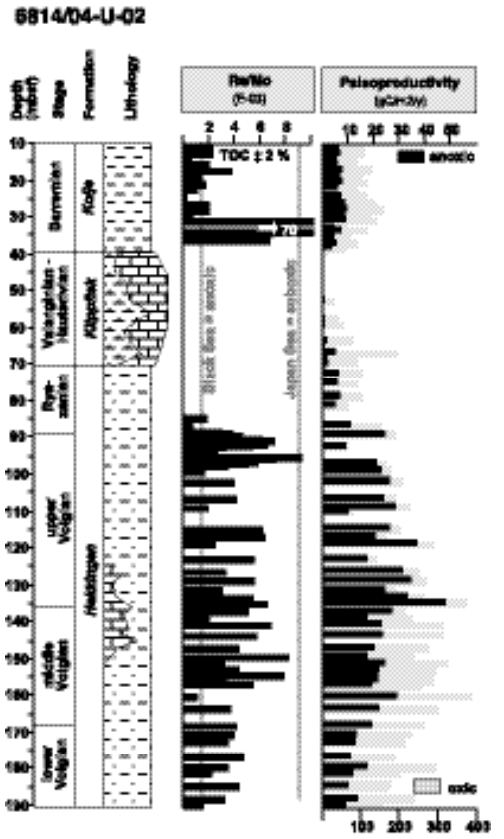

Fig. 4-12 Re/Mo ratios (Lipinski et al., 2003) to discriminate anoxic from dysoxic or oxic environments and paleoproductivity estimates for both oxic (gray) and anoxic (black) conditions for core 6814/04-U-02.

This is also a strong indication that organic carbon accumulation is primarily owing to preservation under anoxic conditions, and that anoxia was very unlikely caused by high productivity, such as it may occur in upwelling areas (Thiede and Van Andel, 1977, Demaison and Moore, 1980; Brumsack, 1980, 1987). As a consequence, paleoproductivities calculated after equation (1) are not appropriate for core 6307/07-U-02. Using equation (2) surface water productivity during black shale formation in core 6814/04-U-02 may have reached 10 to 30 $gC/m^2/y$ (Fig. 4-12), which is comparable to the other core. But TOC/SR relationship (cf. Fig. 4-10) and Re/Mo ratios indicate that the black shales were unlikely deposited in an anoxic, but in a

much more dysoxic environment (Fig. 4-12). Therefore, paleoproductivities calculated after equation (1) appear more realistic. Assuming these conditions, surface water productivity calculated for sediments ≥ 2 wt.% TOC may now reach 200 to 350 gC/m^2/y, which fall in the range of values for modern upwelling areas (250 – 300 gC/m^2/y) (e.g. Pinet, 1992; Romankevich, 1984; Tissot and Welte, 1984). Considering a reduction of these values because deep-water conditions were not fully oxic but dysoxic, similarities exist to average paleoproductivities of marginal upwelling sites off NW-Africa (100 – 300 gC/m^2/y) (e.g. Stein et al., 1989a; Stein, 1991). The results suggest that organic carbon accumulation has been primarily enhanced by an elevated downflux of organic carbon in a high-productive environment (e.g. Pedersen and Calvert, 1990). However, the paleoceanographic position was likely more exposed than restricted (Fig. 4-13), which probably resulted in higher sedimentation rates (higher Ti/Al ratios), higher clastic dilution (lower TOC) and lesser preservation of the lipid-rich OM (lower SRP).

4.5. Summary

Conclusions drawn from all previous microscopic, geochemical, and sedimentological results allow to suggest oceanographic positions for the cores, situated in the margin of the nascent Norwegian Sea (Fig. 4-13). The organic matter in the Ribban Basin site is derived from both marine and terrestrial sources, and the relatively high abundance of recycled “woody” material may reflect a higher degree of oxygenation in the water column and a more energetic (exposed) environment. Although the source rock potential is considerably lower (organic facies BC and C) compared to the Hitra Basin site, its variation through time is reflected by the variations in the amount of primary algae, with some uncertain contributions from recycled marine organic matter. This suggests that primary production in the surface water has probably a distinct control on organic carbon accumulation. Since Re/Mo ratios and TOC/SR relationships support more dysoxic to oxic conditions, estimated surface water productivities are relatively high. The influence of coastal upwelling under oxic to dysoxic deep-water conditions at this site is therefore very likely. This environment results in lower preservation of marine OM, enrichment in refractory OM, and a much lower source rock potential. Large comparability exists to the late

Cenozoic ODP site 658 from the marginal upwelling off NW-Africa, suggesting that black shale formation in the Ribban Basin site was likely a modification of the “productivity model”.

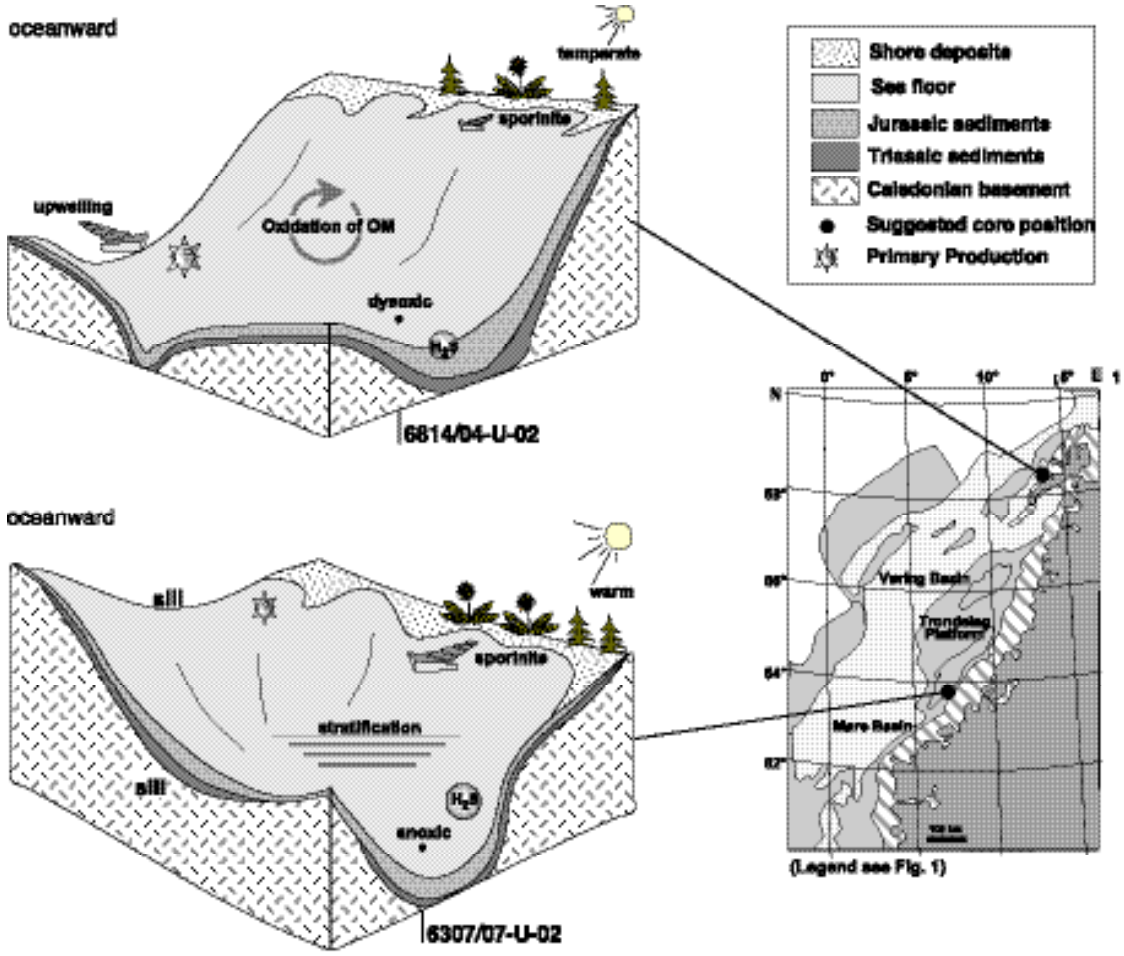

Fig. 4-13 Model for two principally different environments during black shale formation concluded from multiple evidence, suggesting conditions similar to the “stagnation model” for core 6307/07-U-02 and conditions according to the “productivity model” for core 6814/04-U-02. The model does not account for sea-level changes that affect both cores contemporaneously (see Fig. 2, 7).

The sediments from the Hitra Basin site are characterized by higher amounts of marine and lipid-rich terrigenous organic matter compared to the Ribban Basin site. A high source rock potential (organic facies B and BC) is largely reflected by changes in the amount of recycled marine organic matter. Supported by low Re/Mo ratios and TOC/SR relationships, the black shales were likely formed in an anoxic, probably stratified basin with low sedimentation rates. Therefore, surface water productivity was estimated to be very low compared to modern coastal

environments, which is reported from different Cretaceous black shales. Paleoproductivity values are lower than low-productivity areas in the modern Black Sea, but are similar to the nascent Indian Ocean during the Eocene. Hence, the Hitra Basin site is supposed to represent black shale formation similar to the “stagnation model”.

Acknowledgements

Sintef Petroleum Research (Trondheim) provided all core material and is thanked for their kind co-operation. Jens Matthiessen and (number) reviewers are gratefully acknowledged for their comments that helped to improve this contribution. This work was supported financially by the German Science Foundation (grant STE 412/13-1).